Biological and clinical significance of the YKL-40/osteopontin-integrin β4-p70S6K axis induced by macrophages in early oesophageal squamous cell carcinoma

Urakami, Satoshi ; Koma, Yu-ichiro ; Tsukamoto, Shuichi ; Azumi, Yuki ; Miyako, Shoji ; Kitamura, Yu ; Kodama, Takayuki ; Nishio, Mari ;…

(Citation)
The Journal of Pathology,261(1):55-70

(Issue Date)
2023-09

(Resource Type)
journal article

(Version)
Version of Record

Journal of Pathology
J Pathol September 2023; **261**: 55–70
Published online 12 July 2023 in Wiley Online Library
(wileyonlinelibrary.com) DOI: 10.1002/path.6148

ORIGINAL ARTICLE

Biological and clinical significance of the YKL-40/osteopontin–integrin β4–p70S6K axis induced by macrophages in early oesophageal squamous cell carcinoma

Satoshi Urakami[1,2], Yu-ichiro Koma[1]*, Shuichi Tsukamoto[1], Yuki Azumi[1,3], Shoji Miyako[1,3], Yu Kitamura[1,3], Takayuki Kodama[1], Mari Nishio[1], Manabu Shigeoka[1], Hirofumi Abe[2], Yu Usami[4], Yuzo Kodama[2] and Hiroshi Yokozaki[1]

[1] *Division of Pathology, Department of Pathology, Kobe University Graduate School of Medicine, Kobe, Japan*
[2] *Division of Gastroenterology, Department of Internal Medicine, Kobe University Graduate School of Medicine, Kobe, Japan*
[3] *Division of Gastro-intestinal Surgery, Department of Surgery, Kobe University Graduate School of Medicine, Kobe, Japan*
[4] *Department of Oral and Maxillofacial Pathology, Osaka University Graduate School of Dentistry, Osaka, Japan*

**Correspondence to: Y-I Koma, Division of Pathology, Department of Pathology, Kobe University Graduate School of Medicine, 7-5-1 Kusunoki-cho, Chuo-ku, Kobe 650-0017, Japan. E-mail: koma@med.kobe-u.ac.jp*

Abstract

M2 macrophages contribute to the progression of oesophageal squamous cell carcinoma (ESCC); however, the roles of M2 macrophages in early ESCC remain unclear. To clarify the biological mechanisms underlying the interaction between M2 macrophages and oesophageal epithelial cells in early-stage ESCC, *in vitro* co-culture assays between the immortalised oesophageal epithelial cell line Het-1A and cytokine-defined M2 macrophages were established. Co-culture with M2 macrophages promoted the proliferation and migration of Het-1A cells via the mTOR–p70S6K signalling pathway activated by YKL-40, also known as chitinase 3-like 1, and osteopontin (OPN) that were hypersecreted in the co-culture supernatants. YKL-40 and OPN promoted the above phenotypes of Het-1A by making a complex with integrin β4 (β4). Furthermore, YKL-40 and OPN promoted M2 polarisation, proliferation, and migration of macrophages. To validate the pathological and clinical significances of *in vitro* experimental results, immunohistochemistry of human early ESCC tissues obtained by endoscopic submucosal dissection (ESD) was performed, confirming the activation of the YKL-40/OPN–β4–p70S6K axis in the tumour area. Moreover, epithelial expression of β4 and the number of epithelial and stromal infiltrating YKL-40- and OPN-positive cells correlated with the Lugol-voiding lesions (LVLs), a well-known predictor of the incidence of metachronous ESCC. Furthermore, the combination of high expression of β4 and LVLs or high numbers of epithelial and stromal infiltrating YKL-40- and OPN-positive immune cells could more clearly detect the incidence of metachronous ESCC than each of the parameters alone. Our results demonstrated that the YKL-40/OPN–β4–p70S6K axis played important roles in early-stage ESCC, and the high expression levels of β4 and high numbers of infiltrating YKL-40- and OPN-positive immune cells could be useful predictive parameters for the incidence of metachronous ESCC after ESD.

Keywords: integrin β4; early stage; tumour-associated macrophages; metachronous lesion; oesophageal squamous cell carcinoma

Received 14 November 2022; Revised 12 May 2023; Accepted 27 May 2023

No conflicts of interest were declared.

Introduction

Oesophageal cancer is the seventh most commonly occurring cancer worldwide, with an estimated 604,000 new cases in 2020 [1]. Oesophageal squamous cell carcinoma (ESCC) is highly prevalent in East Asia, southern and eastern Africa, and southern Europe [2]. Although the general outcome remains poor for 5-year survival rates, ranging from 15% to 25% [3], the 10-year disease-related survival rate following endoscopic submucosal dissection (ESD) in early superficial ESCC is more than 90% [4]; thus, the detection and treatment of early ESCC are extremely important for improving survival.

ESD is a safe and standard treatment for early ESCC with minimal risk of lymph node metastasis [3]. Despite favourable long-term outcomes of ESD for early ESCC, recurrence (i.e. metachronous ESCC) following ESD could occur in 0.9–9.1% of cases [3]. Lugol-voiding lesions (LVLs) on Lugol chromoendoscopy are known to be associated with high-risk metachronous ESCC [4,5];

however, molecular factors other than LVLs that predict metachronous ESCC have yet to be identified.

The tumour microenvironment consists of cancer cells and stroma, including innate immune cells, and is an active promoter of cancer progression. In the early phase of tumour growth, the interaction between cancer cells and components of the tumour microenvironment supports cancer cell survival and local invasion [6]. Macrophages, which are the main component of immune cells in the tumour microenvironment, have been proposed to differentiate into tumour-suppressive (M1) or tumour-supportive (M2) phenotypes. M2 macrophages are generally characterised by high interleukin (IL)-10 and low IL-12 production and demonstrate high CD163 (a haemoglobin scavenger receptor) and CD204 (a class A macrophage scavenger receptor) expression [7,8]. We previously described how cytokines/chemokines upregulated in the tumour microenvironment, such as C-C motif chemokine ligand 3 and C-X-C motif chemokine ligand 8, promote ESCC progression, using a co-culture system between the TE series ESCC cell lines and peripheral blood monocyte-derived M2 macrophages [9]. Although M2 macrophages could play critical roles in advanced ESCC progression, no report exists on the detailed mechanism of M2 macrophages in early-stage ESCC.

Importantly, previous immunohistochemical reports demonstrated that M2 macrophages could be associated with early-stage ESCC; the number of CD163-positive macrophages in the epithelium increased with high tumour grade in early ESCC [10]; the intraepithelial distribution of CD163- or CD204-positive macrophages in early ESCC was significantly higher than that in the corresponding normal epithelial cells [11]. However, no biological study exists on the role of M2 macrophages in early-stage ESCC. Therefore, we aimed to focus on the interaction between M2 macrophages and oesophageal epithelial cells.

In this study, we established an *in vitro* co-culture system between immortalised oesophageal epithelial squamous cells, Het-1A cells, and cytokine-defined M2 macrophages, and identified the key signalling pathways consisting of cytokines and their receptors that induced proliferation and migration in the Het-1A cells. Furthermore, we investigated whether the activation of these key signalling pathways was involved in early-stage ESCC and analysed their clinical significance by examining their association with metachronous ESCC. These findings could aid in the discovery of useful parameters for determining post-ESD surveillance strategies.

Materials and methods

Ethics approval and patient consent

The Institutional Review Board of Kobe University (B210103) approved all study protocols, and the study was conducted in accordance with the guidelines of the Declaration of Helsinki, 1964. All samples were collected and analysed following prior written informed consent from each patient.

Macrophage culture

The experiment was performed according to previous reports [12,13]. In brief, peripheral blood mononuclear cells (PBMCs) obtained from healthy volunteers were purified using an autoMACS Pro Separator (Miltenyi Biotec, Bergisch Gladbach, Germany). PBMCs were differentiated into macrophages with macrophage colony-stimulating factor (M-CSF) and granulocyte–macrophage colony-stimulating factor (GM-CSF). The macrophages were differentiated using lipopolysaccharide and recombinant human interferon-γ for M1 macrophages, IL-10 for M2 macrophages, and without cytokines for M0 macrophages.

Cell line and cell cultures

The human immortalised oesophageal epithelial cell line Het-1A was obtained from the American Type Culture Collection (Manassas, VA, USA).

Immunohistochemistry (IHC)

IHC was performed on 4-μm-thick sections of paraffin-embedded human and mouse ESCC tissue using the Leica BOND-MAX automated system and BOND Polymer Refine Detection Kit (Leica Biosystems, Bannockburn, IL, USA). The specificity of the integrin β4 (β4) antibody was confirmed using a β4-blocking peptide (Cell Signaling Technology, Beverly, MA, USA) (supplementary material, Figure S1).

Mouse experiments

Mice were maintained at the animal facility of Osaka University Graduate School of Dentistry. All experiments were approved by the Institutional Animal Care and Use Committee (Protocol # 30-007-0 and # 30-007-1) of Osaka University. Six-week-old female C57BL/6 mice treated with 4-nitroquinoline-1-oxide (4NQO) were used for oesophageal carcinogenesis [14].

Additional details and descriptions of Transwell proliferation and migration assays, RT-qPCR, western blotting, phosphokinase array, cytokine array and enzyme-linked immunosorbent assay (ELISA), knockdown of *ITGB4* by siRNA, immunofluorescence, immunoprecipitation (IP), animals and carcinogen treatment, and statistical analysis are provided in Supplementary materials and methods.

Results

The number of infiltrating M2 macrophages in the tumour areas increased in early ESCC

To investigate the potential role of M2 macrophages in early ESCC, we first conducted haematoxylin and

eosin staining and IHC of human early and advanced ESCC tissues (Figure 1A). As previous studies have demonstrated, the number of infiltrating macrophages was high in the invasive areas [9]. Interestingly, the numbers of epithelial and stromal infiltrating immune cells positive for CD68, CD163, and CD204 in the carcinoma *in situ* (CIS) areas were significantly higher than those in the non-tumour areas ($p < 0.01$, Figure 1B). Furthermore, the epithelial infiltrating M2 macrophage ratio, CD163- and CD204-positive cells/CD68-positive cells ratio, increased from 3.3% to 23.5% and from 7.8% to 21.5%, respectively, in the CIS areas compared with the non-tumour areas. Considering these data, we hypothesised that tumour-infiltrating immune cells, including M2 macrophages, could contribute to the progression of early ESCC.

Co-culture of immortalised oesophageal epithelial cells with macrophages promoted proliferation and migration via the mTOR–p70S6K signalling pathway

To investigate the role of macrophages in early-stage ESCC, we established an *in vitro* co-culture system between various polarised macrophages and the immortalised oesophageal epithelial cell line Het-1A. PBMCs were differentiated into macrophages with various polarisations by cytokines (Figure 2A). Consistent with previous reports [7–9,12,13], M2 macrophages showed higher expression of CD163, CD204, and IL-10 and lower expression of IL-12 than did M0 macrophages, while M1 macrophages showed the opposite (supplementary material, Figure S2A,B). In addition, image analysis of immunofluorescence demonstrated that the percentage of CD68-positive cells in the total

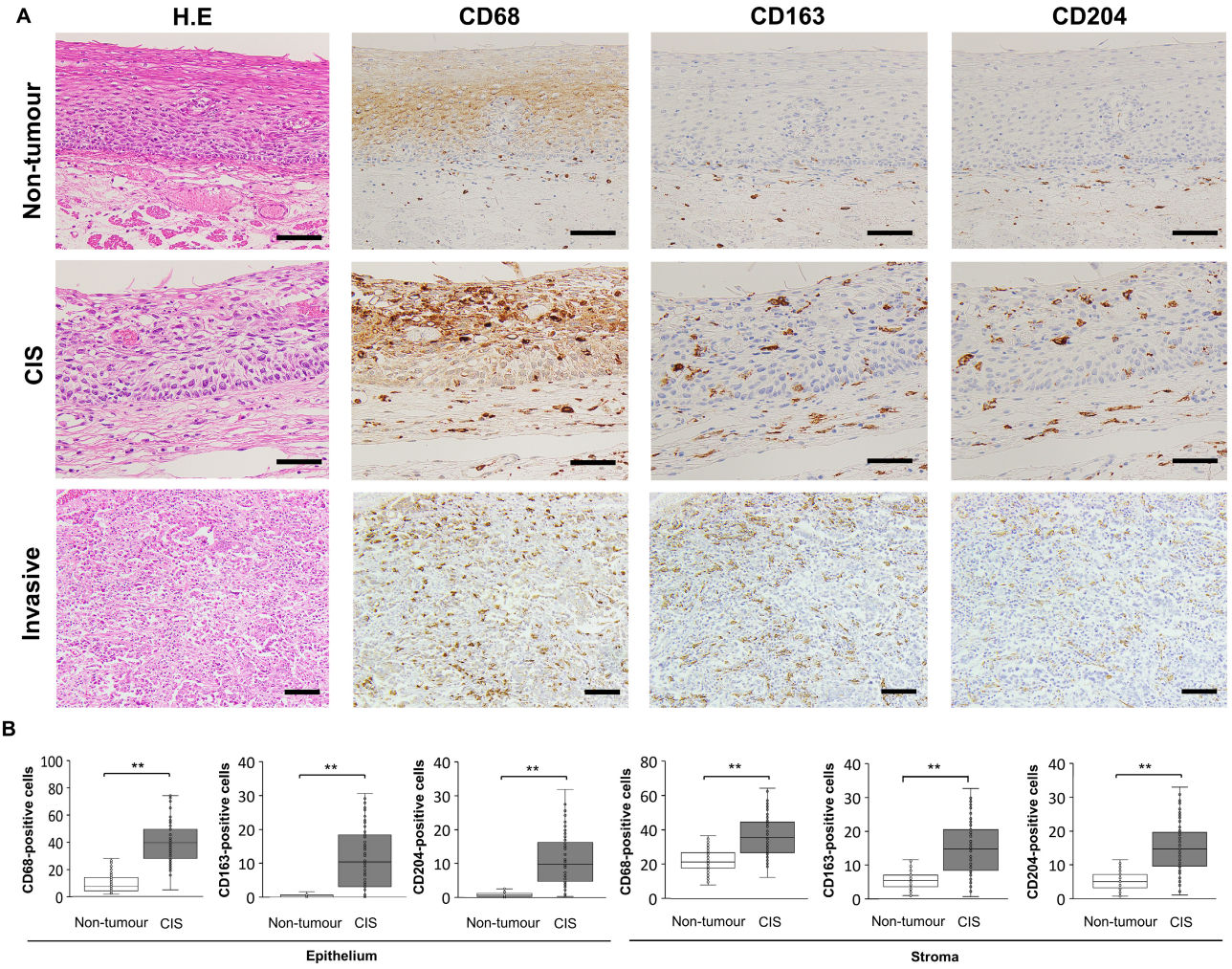

Figure 1. The number of infiltrating M2 macrophages in the tumour areas began to increase from the early stage of oesophageal squamous cell carcinoma (ESCC). (A) Haematoxylin and eosin (H.E) and immunohistochemical staining of epithelial and stromal infiltrating immune cells positive for CD68, CD163, and CD204 in non-tumour and carcinoma *in situ* (CIS) areas and invasive ESCC. Representative images are shown. Scale bar: 100 μm (upper and middle) and 200 μm (lower). (B) Box plots of the epithelial and stromal infiltrating CD68-, CD163-, and CD204-positive immune cell counts in the non-tumour and CIS. To count the numbers of epithelial and stromal infiltrating immune cells, three images were taken in the non-tumour and CIS areas at a magnification of 200×, such that the epithelium and stroma areas were equal in the field of view. The number of infiltrating cells in the box plots is the average of three images in the same patient. Box plots show the medians, first and third quartiles, and maxima and minima of the number of infiltrating cells in 83 early ESCC tissues. The Wilcoxon signed-rank test was performed to compute significance. $^{**}p < 0.01$.

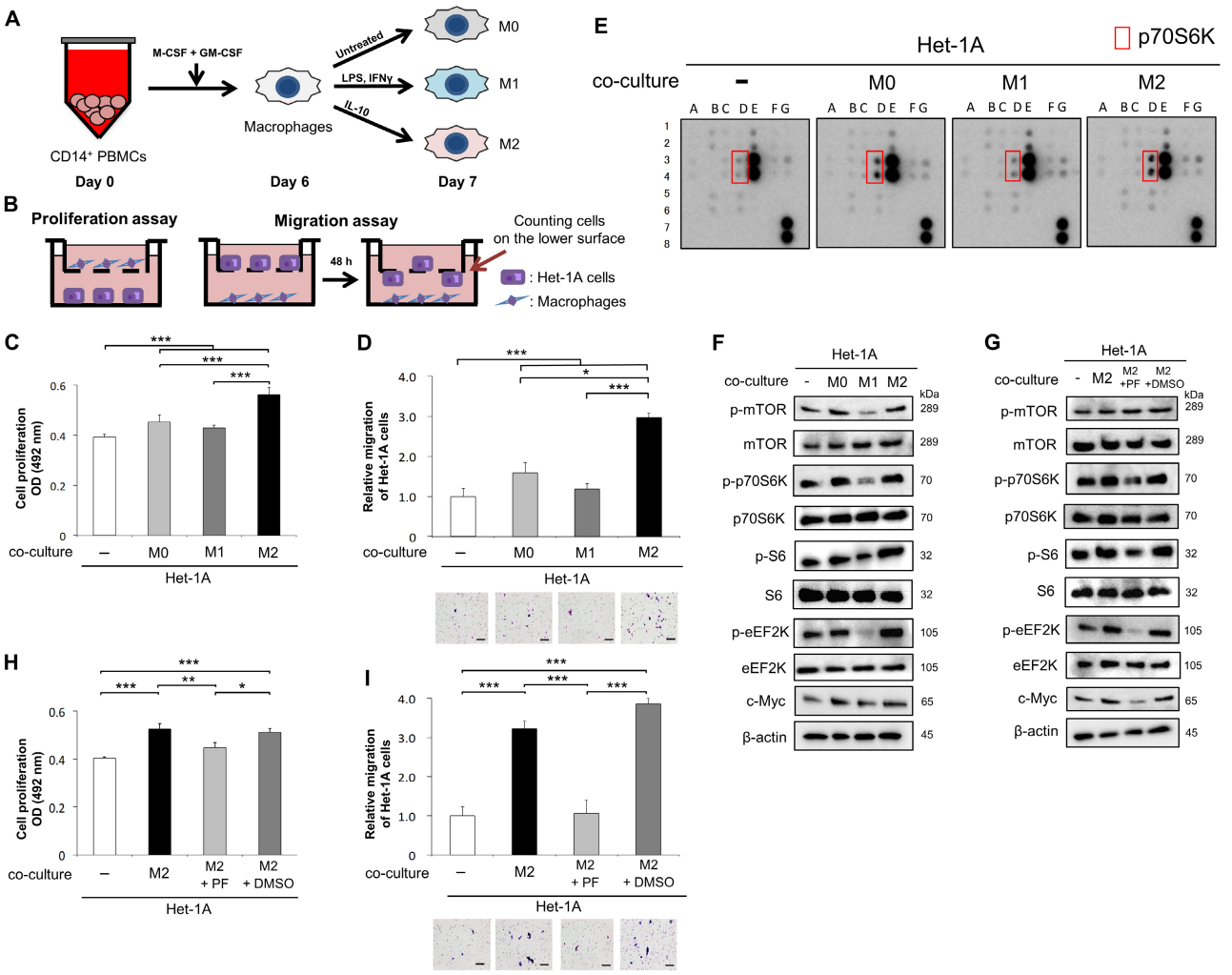

Figure 2. Co-culture with M2 macrophages promoted proliferation and migration via the mTOR–p70S6K signalling pathway in oesophageal epithelial cells. (A) Experimental diagram of the polarisation of peripheral blood monocyte-derived macrophages. Peripheral blood mononuclear cells (PBMCs) were obtained from healthy volunteers. $CD14^+$ PBMCs were purified using an autoMACS Pro Separator and incubated with macrophage colony-stimulating factor (M-CSF) and granulocyte–macrophage colony-stimulating factor (GM-CSF) for 6 days to induce macrophage differentiation. The macrophages were subsequently cultured for 24 h using lipopolysaccharide (LPS) and recombinant human interferon-γ (IFN-γ) for M1 macrophages (M1), IL-10 for M2 macrophages (M2), and without cytokines for M0 macrophages (M0). (B) A schema of the co-culture assay. For the Transwell proliferation assay (left), $CD14^+$ PBMCs (3.0×10^4 cells per well) were differentiated into macrophages with various polarisations in 0.4-μm pore chambers in 24-well plates and co-cultured with Het-1A cells (8.0×10^4 cells per well) in the lower chambers in serum-free medium for 24 h. CellTiter 96 Aqueous One Solution Reagent (Promega, Madison, WI, USA) was added, and absorbance was measured at 492 nm using a microplate reader. For the Transwell migration assay (right), $CD14^+$ PBMCs (8.0×10^4 cells per well) were differentiated into macrophages with various polarisations in the lower chambers of 24-well plates and co-cultured with Het-1A cells (1.5×10^5 cells per well) seeded in 8-μm pore-inserted chambers in serum-free medium. After 48 h, Het-1A cells on the lower surface of the membrane were stained using a Diff-Quik Kit. Five images at 200× magnification were obtained for each membrane using a charge-coupled device camera, and the cells were counted. (C) Transwell proliferation assay to measure the cell proliferation of monocultured Het-1A cells and Het-1A cells co-cultured with M0, M1, and M2. (D) Transwell migration assay of monocultured Het-1A cells and Het-1A cells co-cultured with M0, M1, and M2. (E) Comparison of the levels of various phosphorylated proteins between monocultured Het-1A cells and Het-1A cells co-cultured with M0, M1, and M2 was performed using a phosphokinase array. The red box shows p70S6K spots. (F) Levels of total and phosphorylated mTOR–p70S6K signalling pathway molecules in monocultured Het-1A cells and Het-1A cells co-cultured with M0, M1, and M2 were confirmed by western blotting. β-Actin was used as the loading control. (G–I) Effects of the p70S6K inhibitor (PF4708671, PF) on the mTOR–p70S6K signalling pathway, proliferation, and migration of Het-1A cells were confirmed using (G) western blotting, (H) Transwell proliferation assays, and (I) Transwell migration assays, respectively. Dimethyl sulfoxide (DMSO) was used as a negative control. D and I: representative images are shown. Scale bar: 50 μm. C, D, H, and I: mean ± SD for three independent experiments. $^*p < 0.05$, $^{**}p < 0.01$, $^{***}p < 0.001$; two-sided *t*-test.

number of DAPI-positive cells was nearly 100% in M0, M1, and M2 macrophages (supplementary material, Figure S2C), suggesting that almost all of the PBMCs were differentiated into macrophages [15]. Thereafter, we co-cultured the Het-1A cells with polarised macrophages and observed that co-culture of Het-1A cells with M2 macrophages significantly promoted proliferation and migration compared with monocultured Het-1A cells and co-culture of Het-1A cells with M0 and M1 macrophages (Figure 2B–D). A phosphokinase

array revealed the highest increase in phosphorylated p70S6K (p-p70S6K) in Het-1A cells co-cultured with M2 macrophages compared with that in monocultured Het-1A cells and Het-1A cells co-cultured with M0 and M1 macrophages (Figure 2E and supplementary material, Figure S3A,B). Therefore, we focused on the p70S6K pathway [16,17] and found that in addition to p70S6K, the upstream molecule mTOR and the downstream molecules S6 and eukaryotic elongation factor-2 kinase (eEF2K) were phosphorylated, and the downstream molecule c-Myc was upregulated in Het-1A cells co-cultured with M2 macrophages compared with Het-1A cells monocultured or co-cultured with M0 or M1 macrophages (Figure 2F and supplementary material, Figure S11A). To validate the role of p70S6K in M2 macrophage-induced Het-1A activation, we used a p70S6K inhibitor (PF4708671) and found that the suppression of p70S6K activity inhibited the downstream signalling of p70S6K, proliferation, and migration of Het-1A cells co-cultured with M2 macrophages (Figure 2G–I and supplementary material, Figure S11B). These results suggested that the interaction between oesophageal epithelial cells and M2 macrophages could contribute to early-stage ESCC by activating the mTOR–p70S6K signalling pathway.

YKL-40 and osteopontin (OPN) promoted the proliferation and migration of Het-1A cells via the mTOR–p70S6K signalling pathway

To identify humoral mediators related to the proliferation and migration of Het-1A cells within an indirect co-culture system, we applied the supernatants of Het-1A cell monoculture, M2 macrophage monoculture, and Het-1A/M2 macrophage co-culture to a cytokine array analysis. YKL-40, OPN, and matrix metalloproteinase-9 (MMP-9) spots were significantly increased in the supernatants of Het-1A/M2 macrophage co-culture compared with those of Het-1A monoculture and were abundant in the supernatants of M2 macrophage monoculture (Figure 3A and supplementary material, Figure S4A,B). Many studies have previously reported that MMP-9 plays important roles in the carcinogenesis of ovarian cancer [18], breast cancer [19], and ESCC [20]; therefore, we focused on YKL-40 and OPN. Enzyme-linked immunosorbent assay (ELISA) showed that the co-culture system increased the secretion of YKL-40 and OPN (Figure 3B). Importantly, the secretions of YKL-40 and OPN were not so high in the Het-1A monoculture, whereas YKL-40 and OPN were highly secreted in the M2 macrophage monoculture and even more in the Het-1A/M2 macrophage co-culture. Furthermore, M0 macrophages also secreted YKL-40 and OPN, although the amounts of secretion and the effects of co-culture with the M0 macrophages were smaller than those in the case of M2 macrophages (Figure 3C). To examine whether YKL-40 and OPN contributed to ESCC progression via the mTOR–p70S6K signalling pathway, we treated Het-1A cells with recombinant human YKL-40 (rhYKL-40) and rhOPN and found that YKL-40 and OPN significantly induced mTOR–p70S6K signal activity, proliferation, and migration of Het-1A cells (Figure 3D–F and supplementary material, Figure S11C). In addition, we suppressed *RPS6KB1* mRNA in the Het-1A cells by RNA interference and confirmed the silencing of *RPS6KB1* (supplementary material, Figure S5A,B). The knockdown of *RPS6KB1* in the Het-1A cells cancelled the mTOR–p70S6K signal activation, proliferation, and migration induced by rhYKL-40 and rhOPN (supplementary material, Figures S5C–E and S11D). Furthermore, to compare the effects of YKL-40 and OPN on the Het-1A cells with ESCC cell lines, the poorly or moderately differentiated ESCC cell lines TE-9 or TE-11 were used as a non-tumourigenic or a tumourigenic ESCC because they were not transplantable or were transplantable cancer cells in nude mice, respectively. YKL-40 and OPN promoted proliferation and migration via the mTOR–p70S6K signalling pathway in both of the ESCC cell lines compared to the Het-1A cells; the enhanced effects of proliferation and migration were higher in the tumourigenic TE-11 cells than in the non-tumourigenic TE-9 cells (supplementary material, Figures S6A–C and S11E).

The YKL-40/OPN–β4–p70S6K axis promoted proliferation and migration of Het-1A cells

We further investigated the receptors of YKL-40 and OPN in the Het-1A cells. Well-known receptors of YKL-40 are IL-13Rα2 and the coordination of syndecan-1 and integrin αvβ3 through binding heparin sulphate chains of syndecan-1 on the cell surface [21,22]. OPN acted on various receptors, such as CD44 or integrins including α4β1, α5β1, αvβ1, αvβ3, αvβ5, and α9β1 [23,24]. The commonly involved receptors of both YKL-40 and OPN were integrin families; therefore, we focused on integrins and performed a comprehensive analysis of integrins in the Het-1A cells co-cultured with various polarised macrophages to determine the integrins involved in the progression of early ESCC with YKL-40 and OPN. Alterations in the expression level of β4 integrin protein were similar to the patterns of activated mTOR–p70S6K signalling pathway molecules (Figure 4A), suggesting that β4 integrin could be an important receptor for interaction with the macrophages in the Het-1A cells. Furthermore, a previous study demonstrated that the expression levels of α6β4 were upregulated in ESCC [25], which supported our results; however, no report has demonstrated the interaction between β4 and YKL-40 or OPN. Interestingly, co-culture with M2 macrophages enhanced the co-localisation between YKL-40 or OPN and β4 compared with monoculture in Het-1A cells (supplementary material, Figure S7A–D). Furthermore, a binding assay using immunoprecipitation and immunofluorescence demonstrated the molecular interaction of β4 and YKL-40 or OPN in the Het-1A cells (Figure 4B,C). Considered together, YKL-40 and OPN could form a complex with β4. Moreover, the expression of β4 in Het-1A cells was increased by YKL-40 and OPN

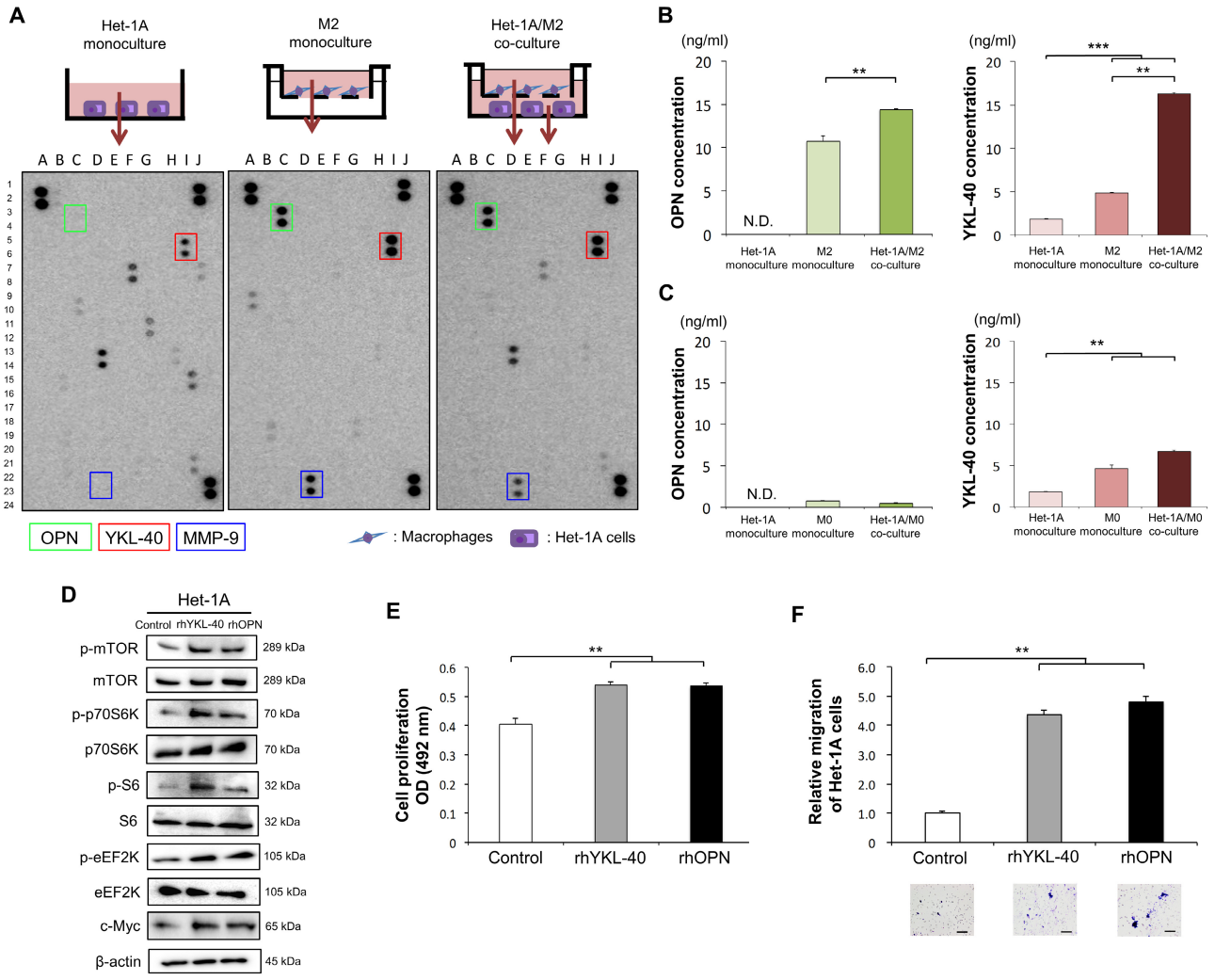

Figure 3. YKL-40 and osteopontin (OPN) promoted the proliferation and migration of oesophageal epithelial cells via the mTOR–p70S6K signalling pathway. (A) Cytokine array of supernatants of Het-1A cell monoculture, M2 macrophage (M2) monoculture, and Het-1A/M2 co-culture. Het-1A cells (3.0×10^5 cells per well) and M2 (1.5×10^5 cells per well) were monocultured for 24 h in serum-free medium, and the supernatants were used for the cytokine array. Het-1A cells (3.0×10^5 cells per well) were co-cultured with M2 (1.5×10^5 cells per well) indirectly for 24 h in serum-free medium, and the supernatant of the upper and lower chambers was used for the cytokine array. The green, red, and blue boxes represent OPN, YKL-40, and MMP-9, respectively. (B) Supernatants of Het-1A cell monoculture, M2 monoculture, and Het-1A/M2 co-culture were analysed using enzyme-linked immunosorbent assay (ELISA) for the secretion levels of YKL-40 and OPN. (C) Supernatants of Het-1A cell monoculture, M0 monoculture, and Het-1A/M0 co-culture were analysed using ELISA for the secretion levels of YKL-40 and OPN. (D) Representative western blots of the components in the mTOR–p70S6K signalling pathway. Het-1A cells were cultured in serum-free medium with or without recombinant human YKL-40 (rhYKL-40) or rhOPN for 24 h. β-Actin was used as the loading control. (E) Proliferation assays of the effects of rhYKL-40 and rhOPN. Het-1A cells were cultured in serum-free medium with or without rhYKL-40 or rhOPN for 24 h, and then the absorbance was measured at 492 nm using a microplate reader. (F) Transwell assay of the effects of rhYKL-40 and rhOPN on the migration of Het-1A cells. Het-1A cells were cultured in the upper chamber in serum-free medium with or without rhYKL-40 or rhOPN for 48 h, and the migrating cells were counted in five randomly chosen fields. Representative images are shown. Scale bar: 50 μm. B, C, E, and F: mean ± SD for three independent experiments. $^{**}p < 0.01$, $^{***}p < 0.001$. N.D., not detected.

(Figure 4D). To clarify whether YKL-40 and OPN affect the proliferation and migration of Het-1A cells via β4, we suppressed *ITGB4* mRNA in the Het-1A cells by RNA interference and confirmed the silencing of *ITGB4* (Figure 4E,F and supplementary material, Figure S8A,B). The knockdown of *ITGB4* in Het-1A cells cancelled the mTOR–p70S6K signal activation, proliferation, and migration induced by rhYKL-40 and rhOPN (Figure 4G–J and supplementary material, Figures S8C–E and S11F,G). Collectively, these results suggested that YKL-40 and OPN making a complex with β4 could activate the mTOR–p70S6K signal pathway in early ESCC.

YKL-40 and OPN promoted M2 polarisation, proliferation, and migration of macrophages

To explore the effects of YKL-40 and OPN on macrophages, PBMC-derived macrophages were treated with rhYKL-40, rhOPN, and IL-10, as shown in Figure 5A. We confirmed that the YKL-40- and OPN-treated macrophages acquired M2 properties, CD163 high, CD204

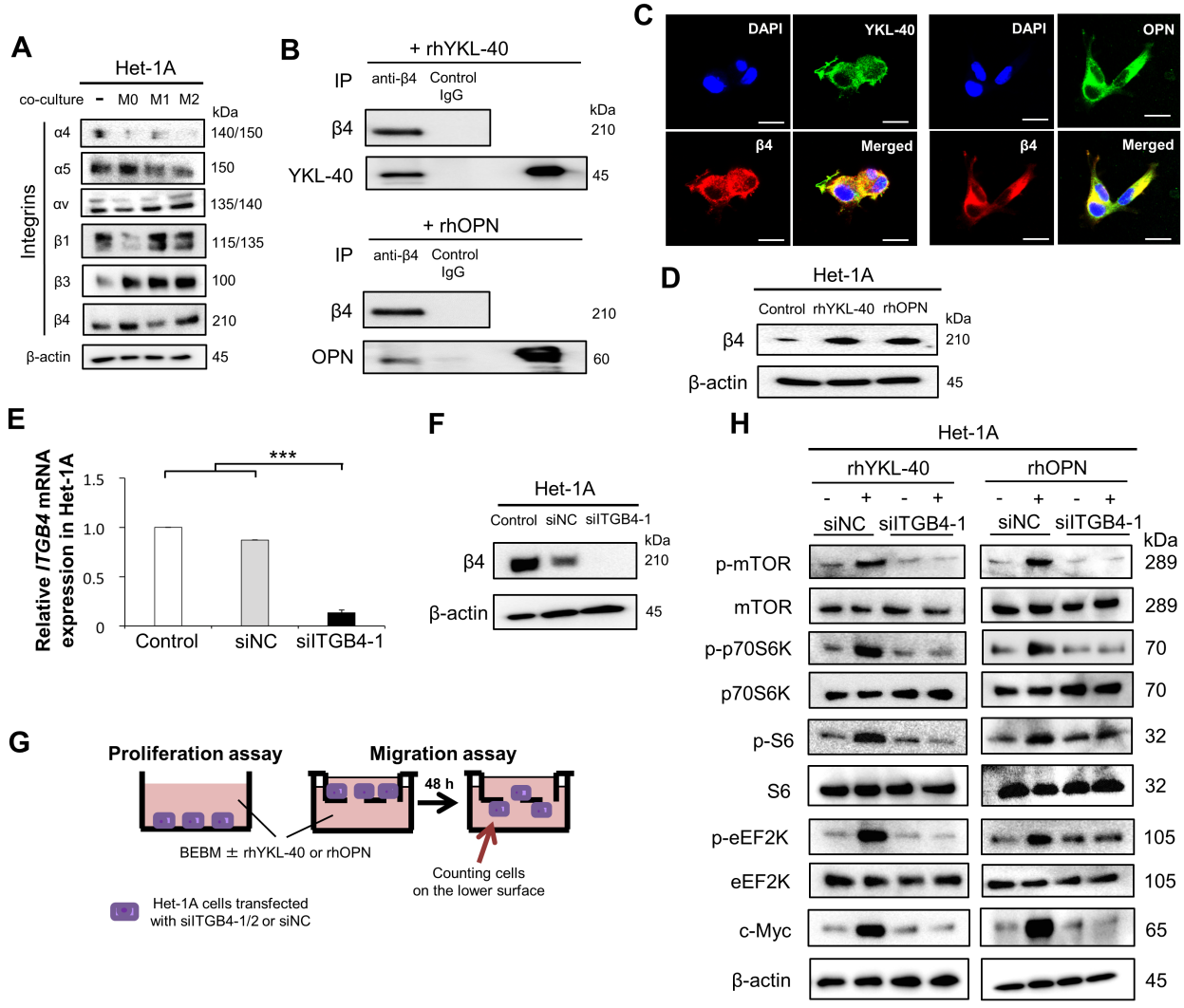

Figure 4 Legend on next page.

high, IL-10 high, and IL-12 low, compared with non-treated macrophages; however, macrophages treated with IL-10, a well-known M2 polarisation factor, acquired the highest M2 property based on quantitative real-time PCR (Figure 5B) and western blotting (Figure 5C). Furthermore, YKL-40 and OPN promoted the proliferation and migration of macrophages (Figure 5D,E). These results indicated that YKL-40 and OPN could mediate the crosstalk between oesophageal epithelial cells and macrophages.

Based on these *in vitro* experiments, we proposed the model shown in Figure 5F. YKL-40 and OPN secreted by M2 macrophages and Het-1A cells activated the mTOR–p70S6K signalling pathway by producing a complex with β4 and subsequently promoted the proliferation and migration of Het-1A cells. YKL-40 and OPN promote M2 polarisation, proliferation, and migration of macrophages. Hence, interactions between oesophageal epithelial cells and macrophages might play important roles in early ESCC.

High expression levels of β4 and p-p70S6K correlated with the high numbers of infiltrating immune cells positive for CD204, YKL-40, and OPN in early ESCC tissues

To validate the results of the *in vitro* experiments, we performed immunohistochemical analysis of YKL-40, OPN, β4, and p-p70S6K in early ESCC human tissues. The numbers of epithelial and stromal infiltrating immune cells positive for YKL-40 and OPN in the tumour areas were significantly higher than those in the non-tumour areas ($p < 0.01$; Figure 6A). Moreover, using double immunofluorescence, we confirmed that the infiltrating immune cells positive for YKL-40 and OPN included CD204-positive macrophages (Figure 6B). Furthermore, we divided the epithelial and stromal infiltrating immune cells positive for CD68, CD163, CD204, YKL-40, and OPN in the tumour areas into high and low groups based on the median number of infiltrating cells (Figure 6C, left). The tumour cells were divided into high- and low-intensity groups based on the intensities of p-p70S6K and β4 (Figure 6C, right). The expression levels of β4 and p-p70S6K significantly correlated with the high numbers of infiltrating epithelial and stromal cells positive for CD204, YKL-40, and OPN (supplementary material, Table S1). Furthermore, in the mouse oesophageal carcinogenesis model using 4NQO, the numbers of infiltrating CD204-, YKL-40-, and OPN-positive cells and the expression levels of β4 were increased as ESCC progressed (supplementary material, Figure S9A–C).

The expression levels of p-p70S6K and β4 and the numbers of infiltrating immune cells positive for CD204, YKL-40, and OPN in early ESCC correlated with the clinicopathological factors

We investigated whether the number of infiltrating immune cells was significantly associated with the clinicopathological factors in patients with early ESCC and found that a high number of epithelial and stromal infiltrating immune cells positive for CD204 significantly correlated with metachronous ESCC ($p = 0.033$; Table 1). Interestingly, high expression levels of β4 also significantly correlated with metachronous ESCC and LVLs ($p = 0.007$ and 0.042, respectively; Table 2). Metachronous ESCC is a clinically important factor since the follow-up period following ESD could be determined; thus, we focused on metachronous ESCC. A high number of epithelial and stromal infiltrating immune cells positive for YKL-40 and OPN significantly correlated with metachronous ESCC (supplementary material, Table S2). Kaplan–Meier analysis revealed that patients with a high number of epithelial and stromal infiltrating immune cells positive for CD204, YKL-40, and OPN had a significantly higher probability of

Figure 4. The YKL-40/osteopontin (OPN)–integrin β4 (β4)–p70S6K axis promoted proliferation and migration of oesophageal epithelial cells. (A) For a comprehensive comparison of the pattern of expression levels of integrins in the Het-1A cells monoculture and Het-1A cells co-cultured with M0 macrophages (M0), M1 macrophages (M1), and M2 macrophages (M2), western blot analysis was performed. Representative western blots of α4, α5, αv, β1, β3, and β4 in the Het-1A cells monoculture and Het-1A cells co-cultured with M0, M1, and M2 indirectly in serum-free conditions for 24 h are shown. (B) Binding assay using immunoprecipitation (IP) demonstrated the molecular interaction of β4 and YKL-40 or OPN in Het-1A cells. Lysates from Het-1A cells were incubated separately with antibodies against β4 and control IgG. Components of the immunoprecipitate were treated using recombinant human YKL-40 (rhYKL-40) or rhOPN and subsequently analysed by western blotting for β4, YKL-40, and OPN. The rightmost lane is rhYKL-40 or rhOPN applied as a control for western blotting. (C) Immunofluorescence of YKL-40 or OPN (green) and β4 (red) in Het-1A cells treated with rhYKL-40 or rhOPN for 24 h. The nuclei were stained with DAPI (blue). The yellow signal in the merged images indicates co-localisation between YKL-40 or OPN and β4. Scale bar: 20 μm. (D) Western blotting for β4 in Het-1A cells treated with or without rhYKL-40 or rhOPN. (E, F) Het-1A cells were transfected with 20 nM siRNA targeting *ITGB4* (siITGB4-1). The efficiency of *ITGB4* knockdown in Het-1A cells was evaluated using (E) RT-qPCR and (F) western blotting. Negative control siRNA (siNC) was used as a negative control. (G) A schema of the silencing assay using siRNA targeting *ITGB4*. For the proliferation assay (left), Het-1A cells (1.0×10^4 cells per well) transfected with siITGB4-1/2 or siNC were seeded in bronchial epithelial cell basal medium (BEBM) with or without rhYKL-40 or rhOPN in 96-well plates. CellTiter 96 Aqueous One Solution Reagent (Promega) was added, and after 24 h, absorbance was measured at 492 nm using a microplate reader. For the migration assay (right), Het-1A cells (1.5×10^5 cells per well) transfected with siITGB4-1/2 or siNC were seeded in 8-μm pore-inserted chambers of 24-well plates with or without rhYKL-40 or rhOPN in BEBM. After 48 h, Het-1A cells on the lower surface of the membrane were stained using a Diff-Quik Kit. Five images at 200× magnification were obtained for each membrane using a charge-coupled device camera, and the cells were counted. (H–J) The effects of rhYKL-40 and rhOPN in the mTOR–p70S6K signalling pathway (H), proliferation assay (I), and Transwell migration assay (J). Representative images are shown. Scale bar: 50 μm (J). In A, D, F, and H, β-actin was used as the loading control. E, I, and J: mean ± SD for three independent experiments. $^{**}p < 0.01$, $^{***}p < 0.001$. N.S., not significant.

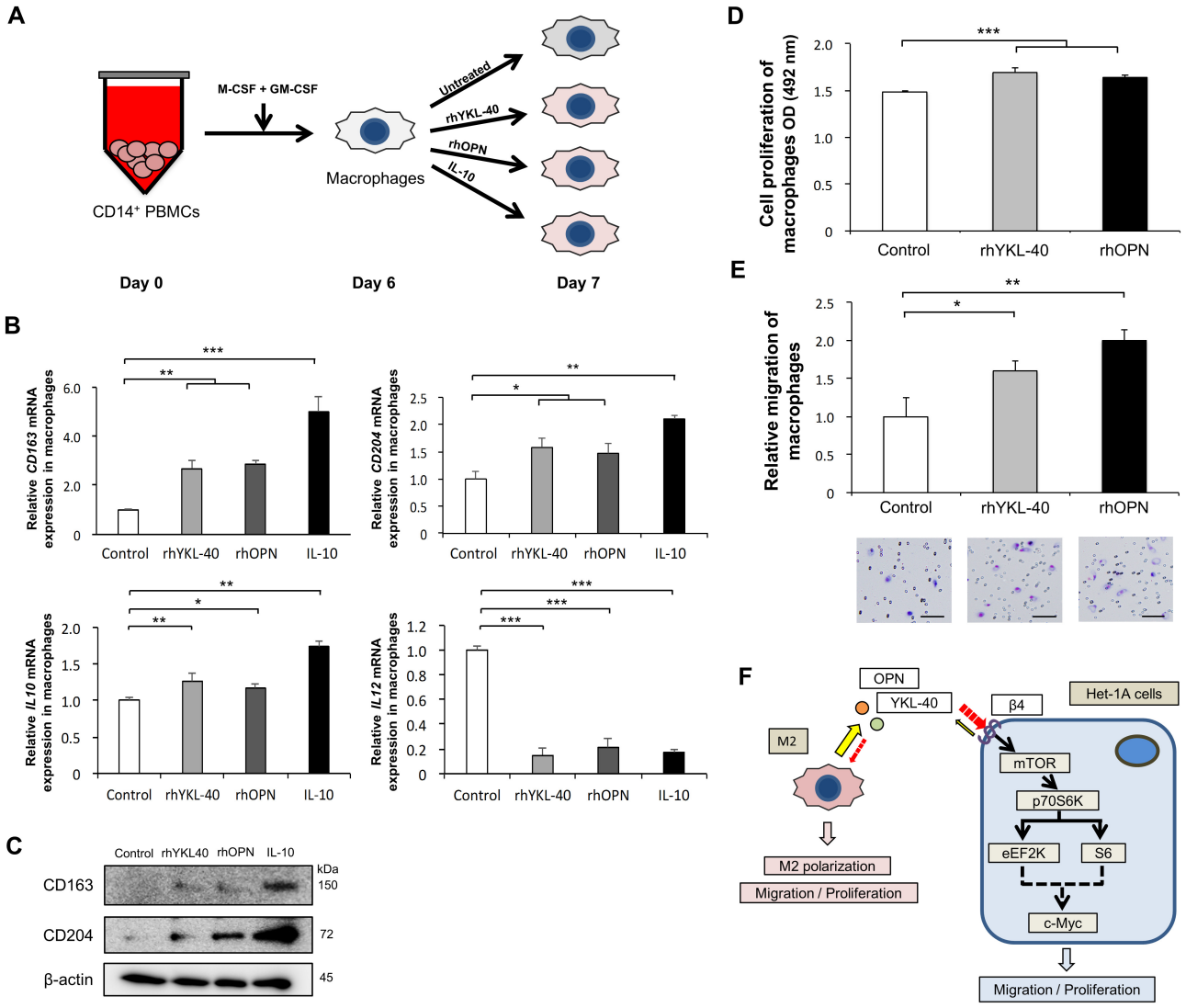

Figure 5. YKL-40 and osteopontin (OPN) promoted M2 polarisation, proliferation, and migration of macrophages. (A) Experimental diagram of YKL-40 and OPN treatment in peripheral blood monocyte-derived macrophages. Peripheral blood mononuclear cells (PBMCs) were obtained from healthy volunteers. $CD14^+$ PBMCs were purified using an autoMACS Pro Separator and incubated with macrophage colony-stimulating factor (M-CSF) and granulocyte–macrophage colony-stimulating factor (GM-CSF) for 6 days to induce macrophage differentiation. The macrophages were subsequently cultured for 24 h with recombinant human YKL-40 (rhYKL-40), rhOPN, and interleukin-10 (IL-10), and without recombinant protein for untreated control. (B and C) Polarisation of macrophages treated with or without rhYKL-40, rhOPN, or IL-10 was confirmed using (B) RT-qPCR and (C) western blotting. *GAPDH* and β-actin were used as the loading control for RT-PCR and western blotting, respectively. (D) Proliferation assay of the effects of rhYKL-40 and rhOPN. Macrophages (8.0×10^4 cells per well) were cultured in serum-free medium with or without rhYKL-40 or rhOPN for 24 h in 24-well plates, and thereafter the absorbance was measured at 492 nm using a microplate reader. (E) Transwell assay of the effects of rhYKL-40 and rhOPN on the migration of macrophages. Macrophages (4.0×10^4 cells per well) were cultured in the upper chamber in serum-free medium with or without rhYKL-40 or rhOPN for 48 h in 24-well plates. Migrating cells were counted in five randomly chosen fields. Representative images are shown. Scale bar: 50 μm. (F) Summary schema of *in vitro* experiments showing that YKL-40 and OPN secreted by M2 macrophages (M2) and Het-1A cells activate the mTOR–p70S6K signalling pathway via integrin β4 (β4), subsequently promoting proliferation and migration in Het-1A cells. YKL-40 and OPN promote M2 polarisation, proliferation, and migration of macrophages. The black dashed arrows indicate the potential mechanism. Red dashed and yellow arrows indicate functional and secreted mechanisms, respectively. B, D, and E: mean ± SD for three independent experiments. $^*p < 0.05$, $^{**}p < 0.01$, $^{***}p < 0.001$.

metachronous ESCC (Figure 6D and supplementary material, Figure S10). In addition, the incidence of metachronous ESCC was significantly associated with the expression level of β4 in tumour cells and LVLs ESCC (L-ESCC) (Figure 6E). Importantly, the combination of high expression levels of β4 and L-ESCC or high numbers of epithelial and stromal infiltrating YKL-40- and OPN-positive immune cells could more clearly predict a high probability of metachronous ESCC (Figure 6F).

Discussion

Consistent with our IHC results, previous immunohistochemical reports have demonstrated that M2 macrophages

could be correlated with early-stage ESCC progression [10,11,26]. Interestingly, one biological study reported that a co-culture of immortalised non-tumourigenic human prostatic epithelial cell lines with the human monocytic leukaemia cell line induced prostate tumourigenesis via androgen receptor-mediated CCL4–STAT3 activation [27]. This study demonstrated that a co-culture system using immortalised epithelial cells could be useful for analysing the mechanism of early-stage cancer. Therefore, we established an *in vitro* co-culture

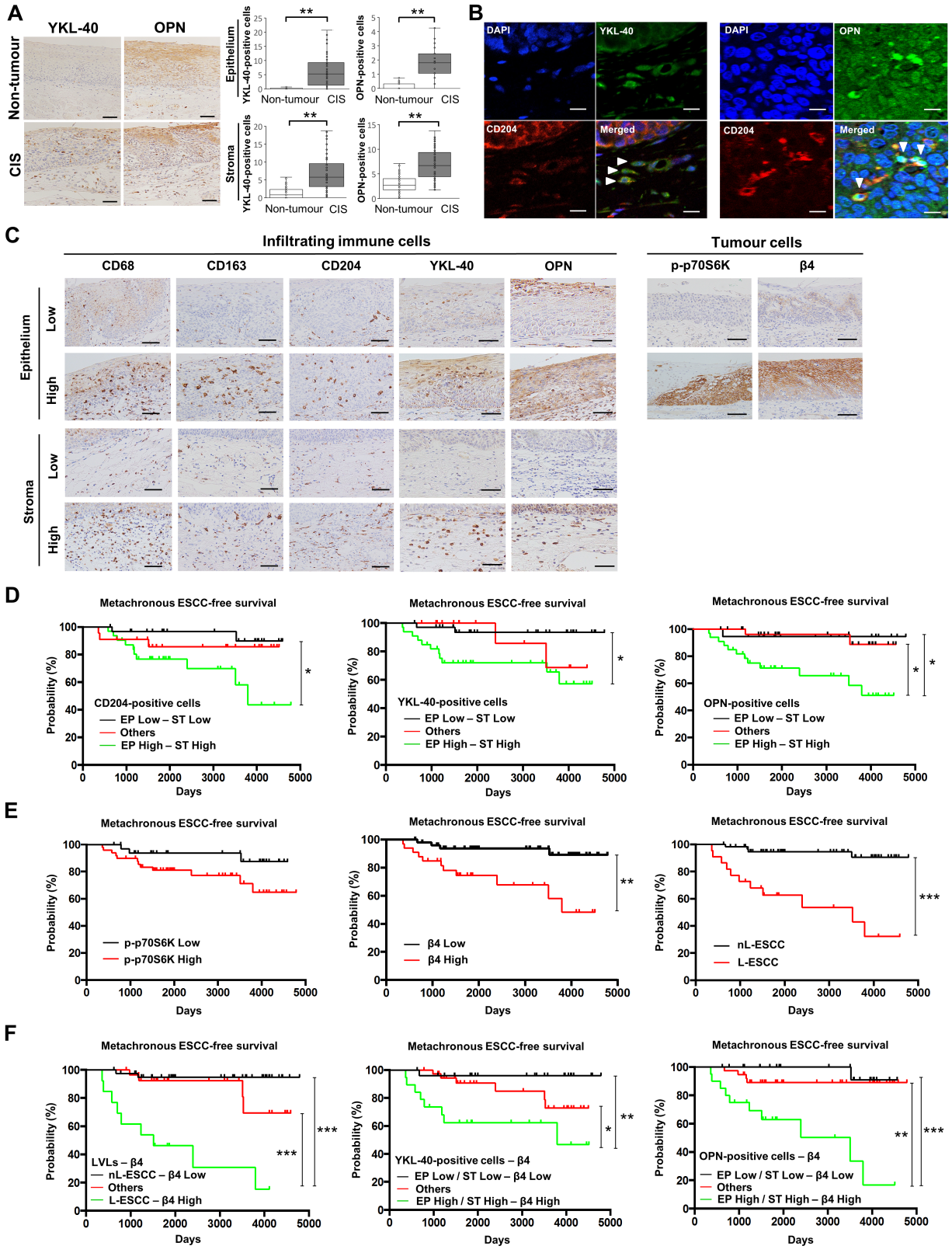

Figure 6 Legend on next page.

system between the immortalised non-tumourigenic oesophageal squamous epithelial cell line Het-1A and cytokine-defined M2 macrophages and identified that activation of the YKL-40/OPN–β4–p70S6K axis revealed by the co-culture analysis was observed in actual early ESCC tissues. This result indicated that our co-culture system was a useful model for analysing the microenvironment of early-stage ESCC.

YKL-40, a secreted glycoprotein belonging to glycoside hydrolase family 18, is synthesised and secreted by various cells, including macrophages, neutrophils, and tumour cells [21,22]. Previous reports have demonstrated that the YKL-40 concentration in the serum of patients with ESCC was significantly associated with shorter overall survival [28]; that higher expression of YKL-40 was associated with the mTOR–p70S6K pathway in glioblastoma [29]; that YKL-40 secreted by M2 macrophages promoted gastric and breast cancer metastasis [30]; and that high expression of YKL-40 was associated with high tumour grade in early-stage epithelial ovarian cancer [31]. OPN is a bone sialoprotein involved in osteoclast attachment to the mineralised bone matrix and plays an important role in cancer progression [23,24]. OPN was critical for hyperactive mTOR-induced tumourigenesis in advanced oral squamous cell carcinoma [32] and regulated the mTOR–p70S6K pathway in breast cancer [24], and the co-existence of OPN and M2 macrophages promoted tumourigenesis in gastric cancer [33]. In premalignant lesions, OPN promoted preneoplastic keratinocyte proliferation and survival via the mitogen-activated protein kinase (MAPK) pathway [34]. Although YKL-40 and OPN promoted tumourigenesis in various cancers, including premalignant lesions, via the mTOR–p70S6K or MAPK pathway, no biological report on early-stage ESCC exists demonstrating that YKL-40 and OPN produced by M2 macrophages could act on ESCC progression through activation of the mTOR–p70S6K pathway.

β4 is a laminin-5 receptor that pairs only with the α6 subunit and results in tumour progression through phosphorylation of the cytoplasmic tail of β4 [35]. Previous reports showed that the heterodimer α6β4 could promote proliferation and invasion of ESCC [25]; β4 expression was enhanced with increasing grade of cervical intraepithelial neoplasia [36]. Regarding the signalling pathway, α6β4 activated PI3K–p70S6K in melanoma [37], and β4 promoted progression via PI3K–mTOR in osteosarcoma [38]. These reports supported our results that the β4–p70S6K axis promoted early-stage ESCC progression. Furthermore, a binding assay using immunoprecipitation of β4 and immunofluorescence demonstrated that YKL-40 and OPN could produce a complex with β4 in Het-1A cells. These findings suggested YKL-40 and OPN as new ligands for the β4-containing complex. Interestingly, the expression level of β4 in the Het-1A cells was upregulated by co-culture with M2 macrophages or by treatment with OPN and YKL-40. β4 could be upregulated by positive feedback from YKL-40 and OPN in the tumour microenvironment. However, the detailed mechanisms remain uncertain, and further studies are warranted.

Although several studies have reported that M2 macrophages expressed YKL-40 and OPN in various cancers [30,33,39], the effects of YKL-40 and OPN on macrophages in early ESCC remain unclear. Our results indicated that YKL-40 and OPN, whose secretion was enhanced by the interaction between M2 macrophages and Het-1A cells, induced the proliferation and migration of Het-1A cells and promoted the proliferation,

Figure 6. Immunohistochemical analysis of infiltrating immune cells and tumour cells in early oesophageal squamous cell carcinoma (ESCC) tissues. (A) Representative images of immunohistochemistry of infiltrating immune cells positive for YKL-40 and osteopontin (OPN) in non-tumour and carcinoma *in situ* (CIS) areas. Box plots of the epithelial and stromal infiltrating YKL-40- and OPN-positive immune cell counts in the non-tumour and CIS areas. To count the numbers of epithelial and stromal infiltrating immune cells, three images were taken in the non-tumour and CIS areas at a magnification of 200×, such that the areas of the epithelium and stroma were equal in the field of view. The numbers of infiltrating cells in the box plots are the average of three images in the same patient. The box plots show medians, first and third quartiles, and maxima and minima of the numbers of infiltrating cells in 83 early ESCC tissues. The Wilcoxon signed-rank test was performed to compute significance. (B) Immunofluorescence of YKL-40 or OPN (green) and CD204 (red) in early ESCC tissues. The nuclei were stained with DAPI (blue). Arrowheads in the merged images indicate cells co-expressing YKL-40 or OPN and CD204. (C) Representative immunohistochemical staining of infiltrating immune cells positive for CD68, CD163, CD204, YKL-40, and OPN, and tumour cells expressing integrin β4 (β4) and phosphorylated p70S6K (p-p70S6K). In the early ESCC tissues, the number of infiltrating immune cells in the epithelium and stroma was divided into low and high groups. The expression levels of β4 and p-p70S6K were stratified into low and high groups based on their immunoreactivity. (D) Correlation of the number of infiltrating immune cells positive for CD204, YKL-40, and OPN in early ESCC tissues with metachronous ESCC-free survival. Kaplan–Meier analysis of metachronous ESCC-free survival in patients with early ESCC, divided into three groups, epithelium (EP) low–stroma (ST) low, EP high–ST high, and others (EP low–ST high and EP high–ST low), using a log-rank test. (E) Correlation of p-p70S6K and β4 expression levels and Lugol-voiding lesions (LVLs) in early ESCC tissues with metachronous ESCC-free survival. Kaplan–Meier analysis of metachronous ESCC-free survival in patients with early ESCC divided into low and high groups according to p-p70S6K and β4 expression, and with no LVLs ESCC (nL-ESCC) or L-ESCC using a log-rank test. (F) Correlation of LVLs and β4 expression in early ESCC tissues with metachronous ESCC-free survival. Kaplan–Meier analysis of metachronous ESCC-free survival in patients with early ESCC divided into three groups, nL-ESCC–β4 low, L-ESCC–β4 high, and others (nL-ESCC–β4 high and L-ESCC–β4 low), using a log-rank test (left). Correlation of the number of infiltrating YKL-40- or OPN-positive immune cells and β4 expression in early ESCC tissues with metachronous ESCC-free survival. Kaplan–Meier analysis of metachronous ESCC-free survival in patients in early ESCC divided into three groups, EP low/ST low–β4 low, EP high/ST high–β4 high, and others (EP low/ST high–β4 low and high, EP high/ST low–β4 high and low, EP low/ST low–β4 high, and EP high/ST high–β4 low), using a log-rank test for YKL-40 (middle) and OPN (right), respectively. A–C: representative images are shown. Scale bar: 100 μm (A, C); 20 μm (B). $^{*}p < 0.05$, $^{**}p < 0.01$, $^{***}p < 0.001$.

Table 1. Correlation between the numbers of infiltrating immune cells and clinicopathological parameters in early oesophageal squamous cell carcinoma (ESCC).

Characteristics	No. of patients	CD68*			*P* value	CD163*			*P* value	CD204*			*P* value
		EP low–ST low ($n = 23$)	Others ($n = 35$)	EP high–ST high ($n = 25$)		EP low–ST low ($n = 34$)	Others ($n = 13$)	EP high–ST high ($n = 36$)		EP low–ST low ($n = 30$)	Others ($n = 22$)	EP high–ST high ($n = 31$)	
Age, years													
< 65	29	5	15	9	0.27	11	4	14	0.82	9	8	12	0.17
≥ 65	54	18	20	16		23	9	22		21	14	19	
Sex													
Male	75	21	31	23	1.00	29	10	36	0.009**	26	18	31	0.029*
Female	8	2	4	2		5	3	0		4	4	0	
Location†													
(Ut/Mt/Lt)	3/66/14	0/17/6	1/28/6	2/21/2	0.33	1/23/10	0/10/3	2/33/1	0.48	0/23/7	0/17/5	3/26/2	0.089
Classification†													
(EP/LPM)	34/49	11/12	14/21	9/16	0.69	15/19	4/9	15/21	0.79	18/12	6/16	10/21	0.029*
Alcohol intake													
Yes	50	10	21	19	0.072	19	5	26	0.079	16	12	22	0.30
No	33	13	14	6		15	8	10		14	10	9	
Smoking status													
Yes	51	13	23	15	0.78	20	7	24	0.69	17	11	23	0.15
No	32	10	12	10		14	6	12		13	11	8	
Horizontal location													
≦1/2	64	20	27	17	0.34	25	10	29	0.83	26	17	21	0.21
>1/2	19	3	8	8		9	3	7		4	5	10	
LVLs‡													
L-ESCC	22	2	11	9	0.056	9	5	8	0.50	7	4	11	0.36
nL-ESCC	61	21	24	16		25	8	28		23	18	20	
Metachronous ESCC§													
Yes	15	3	7	5	0.82	5	1	9	0.83	2	3	10	0.033*
No	68	20	28	20		29	12	27		28	19	21	

*Infiltrating immune cells positive for CD68, CD163, and CD204 in the epithelium (EP) and stroma (ST) were divided into low and high groups based on the median number of infiltrating cells. Patients with early ESCC were divided into three groups: EP low–ST low, EP high–ST high, and others (EP low–ST high and EP high–ST low).

†According to the *Japanese Classification of Oesophageal Cancer* (10th edn) [46]: Ut/Mt/Lt, upper thoracic oesophagus/middle thoracic oesophagus/lower thoracic oesophagus; EP, epithelium; LPM, lamina propria mucosa.

‡More than ten Lugol-voiding lesions (LVLs) per endoscopic view on Lugol chromoendoscopy were defined as LVLs ESCC (L-ESCC) [47]. nL-ESCC, no L-ESCC.

§Metachronous ESCC was defined as ESCC other than local recurrence detected in surveillance oesophagogastroduodenoscopy.

Data were analysed using χ^2 tests; $p < 0.05$ was considered statistically significant; *$p < 0.05$; **$p < 0.01$.

Table 2. Correlation between the expression levels of integrin β4 (β4) and phosphorylated p70S6K (p-p70S6K) and clinicopathological parameters in oesophageal squamous cell carcinoma (ESCC) tissues.

Characteristics	No. of patients	Expression of β4*			Expression of p-p70S6K†		
		Low ($n = 50$)	High ($n = 33$)	*P* value	Low ($n = 34$)	High ($n = 49$)	*P* value
Age, years							
<65	29	15	14	0.35	12	17	1.00
≥65	54	35	19		22	32	
Sex							
Male	75	43	32	0.14	28	47	0.059
Female	8	7	1		6	2	
Location‡							
(Ut/Mt/Lt)	3/66/14	1/41/8	2/25/6	0.59	1/26/7	2/40/7	0.81
Classification‡							
(EP/LPM)	34/49	26/24	8/25	0.014*	17/17	17/32	0.18
Alcohol intake							
Yes	50	29	21	0.65	17	33	0.17
No	33	21	12		17	16	
Smoking status							
Yes	51	24	27	0.003**	15	36	0.011*
No	32	26	6		19	13	
Horizontal location							
≦ 1/2	64	40	24	0.59	26	38	1.00
> 1/2	19	10	9		8	11	
LVLs§							
L-ESCC	22	9	13	0.042*	8	14	0.80
nL-ESCC	61	41	20		26	35	
Metachronous ESCC‖							
Yes	15	4	11	0.007**	3	12	0.086
No	68	46	22		31	37	

*The early ESCC samples were divided into low (scores 1 and 2) and high (score 3) groups based on the immunoreactivity of β4 in tumour areas.
†The early ESCC samples were divided into low and high groups based on the expression levels of p-p70S6K in the tumour areas.
‡According to the *Japanese Classification of Oesophageal Cancer* (10th edn) [46]: Ut/Mt/Lt, upper thoracic oesophagus/middle thoracic oesophagus/lower thoracic oesophagus; EP, epithelium; LPM, lamina propria mucosa.
§More than ten Lugol-voiding lesions (LVLs) per endoscopic view on Lugol chromoendoscopy were defined as LVLs ESCC (L-ESCC) [47]. nL-ESCC, no L-ESCC.
‖Metachronous ESCC was defined as ESCC other than local recurrence detected in surveillance oesophagogastroduodenoscopy.
Data were analysed using χ^2 tests; *$p < 0.05$, **$p < 0.01$.

migration, and M2 polarisation of macrophages. Interestingly, co-culture with M0 macrophages could promote proliferation and migration and upregulate the molecules in the mTOR–p70S6K signalling pathway in the Het-1A cells; however, the amounts of secretion and the effects of co-culture of YKL-40 and OPN in the M0 macrophages were smaller than those in the M2 macrophages, and the effects of proliferation and migration in the M0 macrophages were lower than those in the M2 macrophages. This suggested that M2 macrophages played more important roles in early ESCC progression than did M0 macrophages, and that YKL-40 and OPN played important roles in the crosstalk between M2 macrophages and oesophageal epithelial cells in the tumour microenvironment. Furthermore, ELISA revealed that Het-1A cells do not produce OPN at all; therefore, the recruitment and M2 polarisation of macrophages in early ESCC could be implicated in exogenous OPN secreted by other stromal cells, such as cancer-associated fibroblasts [40], or other humoral factors. Moreover, the ability of YKL-40 and OPN to induce M2 polarisation was lower than that of IL-10, a known M2-inducible factor, suggesting that other factors could induce the recruitment and M2 polarisation of macrophages in the first step of ESCC carcinogenesis; however, our study was unable to elucidate this mechanism.

To validate the *in vitro* experiments, we performed IHC on human and mouse ESCC tissues. In human early ESCC, the high number of infiltrating cells positive for CD204, YKL-40, and OPN in the epithelium and stroma closely correlated with the high expression of p-p70S6K and β4 in the oesophageal epithelial cells. Furthermore, in CIS areas of the mouse model, the numbers of infiltrating CD204-, YKL-40-, and OPN-positive cells and the expression of β4 were higher than in non-tumour areas. These results supported the notion that the interaction between M2 macrophages and oesophageal epithelial cells could induce the YKL-40/OPN–β4–p70S6K axis.

Metachronous ESCC is important for selecting patients who require careful monitoring after ESD. Katada *et al* reported that metachronous ESCC was detected in 24.7% of patients with LVLs within 2 years of the first detection of early ESCC [5]. Although metachronous ESCC was associated with LVLs, molecular factors other than LVLs remain unclear. Our study suggested that epithelial expression of β4 in early ESCC was correlated with LVLs, and the combination of high expression of β4 and LVLs or high numbers of epithelial and stromal infiltrating cells positive for YKL-40 and OPN could more clearly detect the incidence of metachronous ESCC than any of these parameters alone. Therefore, these parameters

could be useful for predicting the incidence of metachronous ESCC.

Considering oncological therapy, a clinical trial of the p70S6K inhibitor in advanced cancers has already been performed [41]. Furthermore, a YKL-40 neutralising antibody and humanised anti-OPN antibody blocked tumour progression in mouse models [42,43]. These studies suggested that inhibitors or antibodies of p70S6K, YKL-40, and OPN could be used as therapeutic agents for preventing the incidence of early-stage ESCC. Therefore, *in vivo* experiments are warranted to confirm whether these inhibitors could prevent early ESCC carcinogenesis in mice treated with 4NQO.

This study has several limitations. First, we used Het-1A cells as a premalignant model. The rationale for using Het-1A cells was as follows: Het-1A cells are not completely normal oesophageal epithelial cells since they are immortalised by the SV40 T antigen [44], and p53 is inactivated in Het-1A cells [45]. In addition, Stoner *et al* demonstrated that Het-1A cells could not form tumours during a period of 1 year after incubation in nude mice [44]. Furthermore, comparison of the effect of rhYKL-40 and rhOPN on Het-1A cells with non-tumourigenic and tumourigenic ESCC cell lines showed that Het-1A cells had properties more similar to non-tumourigenic ESCC than to tumourigenic ESCC. Collectively, we considered it acceptable to use Het-1A cells for the analysis of early-stage ESCC. Second, IHC in the mouse model using 4NQO to induce oesophageal tumourigenesis was performed; however, further studies using inhibitors and genetically engineered mice against this axis are warranted to completely demonstrate the interaction between M2 macrophages and epithelial cells in the progression of early-stage ESCC via the YKL-40/OPN–β4–p70S6K axis. Third, not all infiltrating immune cells positive for YKL-40 and OPN in IHC were macrophages, and distinguishing macrophages from other inflammatory cells was challenging.

In conclusion, we established an *in vitro* co-culture system between cytokine-defined macrophages at various differentiation stages and immortalised oesophageal epithelial cells and revealed that activation of the YKL-40/OPN–β4–p70S6K axis was observed in early-stage ESCC. In addition, the high expression levels of β4 and high numbers of infiltrating YKL-40- and OPN-positive immune cells could be useful predictive parameters to evaluate the incidence of metachronous ESCC after ESD.

Acknowledgements

We acknowledge our colleagues Yumi Hashimoto, Nobuo Kubo, Miki Yamazaki, and Tomoki Fujita for their excellent technical support. This study was supported by Grants-in-Aid for Scientific Research (grant numbers 20K07373 and 22K06978) from the Japan Society for the Promotion of Science. This study was also supported by the Takeda Science Foundation.

Author contributions statement

SU, Y-IK and HY conceptualised the study. SU and Y-IK performed most of the experimental procedures. SU, HA and MN analysed data. SU, Y-IK and HY wrote the original draft and ST, SM, YA, YKi, TK and MS reviewed the manuscript. YU provided the mouse specimens. YKo and HY supervised the study. All the authors read and approved the revised manuscript.

Data availability statement

This published article and its supplementary information files include all the data generated or analysed during this study.

References

1. Sung H, Ferlay J, Siegel R, *et al*. Global cancer statistics 2020: GLOBOCAN estimates of incidence and mortality worldwide for 36 cancers in 185 countries. *CA Cancer J Clin* 2021; **71:** 209–249.
2. Huang FL, Yu SJ. Esophageal cancer: risk factors, genetic association, and treatment. *Asian J Surg* 2018; **41:** 210–215.
3. Xu JQ, Zhang ZC, Chen WF, *et al*. Repeat endoscopic submucosal dissection as salvage treatment for local recurrence of esophageal squamous cell carcinoma after initial endoscopic submucosal dissection. *Gastrointest Endosc* 2022; **96:** 18–27.e1.
4. Hsu MH, Wang WL, Chen TH, *et al*. Long-term outcomes of endoscopic submucosal dissection for superficial esophageal squamous cell carcinoma in Taiwan. *BMC Gastrol* 2021; **21:** 308.
5. Katada C, Yokoyama T, Yano T, *et al*. Alcohol consumption and multiple dysplastic lesions increase risk of squamous cell carcinoma in the esophagus, head, and neck. *Gastroenterology* 2016; **151:** 860–869.
6. Anderson NM, Simon MC. The tumor microenvironment. *Curr Biol* 2020; **30:** R921–R925.
7. Mantovani A, Sozzani S, Locati M, *et al*. Macrophage polarization: tumor-associated macrophages as a paradigm for polarized M2 mononuclear phagocytes. *Trends Immunol* 2001; **23:** 549–555.
8. Wang B, Liu H, Dong X, *et al*. High CD204^{+} tumor-infiltrating macrophage density predicts a poor prognosis in patients with urothelial cell carcinoma of the bladder. *Oncotarget* 2015; **6:** 20204–20214.
9. Yokozaki H, Koma Y, Shigeoka M, *et al*. Cancer as a tissue: the significance of cancer-stromal interactions in the development, morphogenesis and progression of human upper digestive tract cancer. *Pathol Int* 2018; **68:** 334–352.
10. Kumagai Y, Sobajima J, Higashi M, *et al*. Tumor-associated macrophages and angiogenesis in early stage esophageal squamous cell carcinoma. *Esophagus* 2016; **13:** 245–253.
11. Ichihara Y, Yokozaki H. Close association of intraepithelial accumulation of M2-skewed macrophages with neoplastic epithelia of the esophagus. *Kobe J Med Sci* 2021; **67:** E18–E33.
12. Mia S, Warnecke A, Zhang XM, *et al*. An optimized protocol for human M2 macrophages using M-CSF and IL-4/IL-10/TGF-β yields a dominant immunosuppressive phenotype. *Scand J Immunol* 2014; **79:** 305–314.
13. Nielsen MC, Andersen MN, Møller HJ. Monocyte isolation techniques significantly impact the phenotype of both isolated monocytes and derived macrophages *in vitro*. *Immunology* 2019; **159:** 63–74.

14. Han XH, Knudsen B, Bemis D, *et al*. Oral cavity and esophageal cancinogenesis modeled in carcinogen-treated mice. *Clin Cancer Res* 2004; **10:** 301–313.
15. Nishio M, Urakawa N, Shigeoka M, *et al*. Software-assisted morphometric and phenotype analyses of human peripheral blood monocyte-derived macrophages induced by a microenvironment model of human esophageal squamous cell carcinoma. *Pathol Int* 2016; **66:** 83–93.
16. Fenton TR, Gout IT. Functions and regulation of the 70 kDa ribosomal S6 kinases. *Int J Biochem Cell Biol* 2011; **43:** 47–59.
17. Chellini L, Monteleone V, Lombari M, *et al*. The oncoprotein Myc controls the phosphorylation of S6 kinase and AKT through protein phosphatase 2A. *J Cell Biochem* 2018; **119:** 9878–9887.
18. Carroll MJ, Kapur A, Felder M, *et al*. M2 macrophages induce ovarian cancer cell proliferation via a heparin binding epidermal growth factor/matrix metalloproteinase 9 intercellular feedback loop. *Oncotarget* 2016; **7:** 86608–86620.
19. Joseph C, Alsaleem M, Orah N, *et al*. Elevated MMP9 expression in breast cancer is a predictor of shorter patient survival. *Breast Cancer Res Treat* 2020; **182:** 267–282.
20. Li Y, Ma J, Guo Q, *et al*. Overexpression of MMP-2 and MMP-9 in esophageal squamous cell carcinoma. *Dis Esophagus* 2009; **22:** 664–667.
21. Shao R, Hamel K, Petersen L, *et al*. YKL-40, a secreted glycoprotein, promotes tumor angiogenesis. *Oncogene* 2009; **28:** 4456–4468.
22. Zhao T, Su Z, Li Y, *et al*. Chitinase-3 like-protein-1 function and its role in disease. *Signal Transduct Target Ther* 2020; **5:** 201.
23. Zhao H, Chen Q, Alam A, *et al*. The role of osteopontin in the progression of solid organ tumour. *Cell Death Dis* 2018; **9:** 356.
24. Ahmed M, Kundu G. Osteopontin selectively regulates p70S6K/mTOR phosphorylation leading to NF-κB dependent AP-1-mediated ICAM-1 expression in breast cancer cells. *Mol Cell* 2010; **9:** 101.
25. Kwon J, Lee TS, Lee HW, *et al*. Integrin alpha 6: a novel therapeutic target in esophageal squamous cell carcinoma. *Int J Oncol* 2013; **43:** 1523–1530.
26. Weber M, Iliopoulos C, Moebius P, *et al*. Prognostic significance of macrophage polarization in early stage oral squamous cell carcinomas. *Oral Oncol* 2016; **52:** 75–84.
27. Fang LY, Izumi K, Lai KP, *et al*. Infiltrating macrophages promote prostate tumorigenesis via modulating androgen receptor-mediated CCL4-STAT3 signaling. *Cancer Res* 2013; **73:** 5633–5646.
28. Xing S, Zheng X, Zeng T, *et al*. Chitinase 3-like 1 secreted by peritumoral macrophages in esophageal squamous cell carcinoma is a favorable prognostic factor for survival. *World J Gastroenterol* 2017; **21:** 7693–7704.
29. Pelloski CE, Lin E, Zhang L, *et al*. Prognostic associations of activated mitogen-activated protein kinase and Akt pathways in glioblastoma. *Clin Cancer Res* 2006; **12:** 3935–3941.
30. Chen Y, Zhang S, Wang Q, *et al*. Tumor-recruited M2 macrophages promote gastric and breast cancer metastasis via M2 macrophage-secreted CHI3L1 protein. *J Hematol Oncol* 2017; **10:** 36.
31. Lawrensin K, Mhawech-Fauceglia P, Worthington J, *et al*. Identification of novel candidate biomarkers of epithelial ovarian cancer by profiling the secretomes of three-dimensional genetic models of ovarian carcinogenesis. *Int J Cancer* 2015; **137:** 1806–1817.
32. Gan N, Zou S, Hang W, *et al*. Osteopontin is critical for hyperactive mTOR-induced tumorigenesis in oral squamous cell carcinoma. *J Cancer* 2017; **8:** 1362–1370.
33. Lin CN, Wang CJ, Chao YJ, *et al*. The significance of the co-existence of osteopontin and tumor-associated macrophages in gastric cancer progression. *BMC Cancer* 2015; **15:** 128.
34. Luo X, Ruhland MK, Pazolli E, *et al*. Osteopontin stimulates preneoplastic cellular proliferation through activation of the MAPK pathway. *Mol Cancer Res* 2011; **9:** 1018–1029.
35. Steward RL, O'Connor KL. Clinical significance of the integrin α6β4 in human malignancies. *Lab Invest* 2015; **95:** 976–986.
36. Carico E, French D, Bucci B, *et al*. Integrin β4 expression in the neoplastic progression of cervical epithelium. *Gynecol Oncol* 1993; **1:** 61–66.
37. Shaw LM, Rabinovitz I, Wang HH, *et al*. Activation of phosphoinositide 3-OH kinase by the α6β4 integrin promotes carcinoma invasion. *Cell* 1997; **91:** 949–960.
38. Wang Q, Xue L, Shi Z, *et al*. Upregulation of exosomal integrin β4 causes osteosarcoma cell proliferation via the PI3K-Akt-mTOR signaling pathway. *Transl Cancer Res* 2018; **7:** 1209–1220.
39. Cohen N, Shani O, Raz Y, *et al*. Fibroblasts drive an immunosuppressive and growth-promoting microenvironment in breast cancer via secretion of chitinase 3-like 1. *Oncogene* 2017; **31:** 4457–4468.
40. Kariya Y, Kariya Y. Osteopontin in cancer: mechanisms and therapeutic targets. *Int J Transl Med* 2022; **2:** 419–447.
41. Tsimberidou AM, Shaw JV, Juric D, *et al*. Phase 1 study of M2698, a p70S6K/AKT dual inhibitor, in patients with advanced cancer. *J Hematol Oncol* 2021; **14:** 127.
42. Faibish M, Francescone R, Bentley B, *et al*. A YKL-40-neutralizing antibody blocks tumor angiogenesis and progression: a potential therapeutic agent in cancers. *Mol Cancer Ther* 2011; **10:** 742–751.
43. Dai J, Li B, Shi J, *et al*. A humanized anti-osteopontin antibody inhibits breast cancer growth and metastasis in vivo. *Cancer Immunol Immunother* 2010; **59:** 355–366.
44. Stoner GD, Kaighn ME, Reddel RR, *et al*. Establishment and characterization of SV40 T-antigen immortalized human esophageal epithelial cells. *Cancer Res* 1991; **51:** 365–371.
45. Kong J, Nagasawa H, Isariyawongse BK, *et al*. Induction of intestinalization in human esophageal keratinocytes is a multistep process. *Carcinogenesis* 2009; **1:** 122–230.
46. Japan Esophageal Society. *Japanese Classification of Esophageal Cancer* (10th edn). Kanehara & Co: Tokyo, 2008.
47. Matsuno K, Ishihara R, Nakagawa K, *et al*. Endoscopic findings corresponding to multiple lugol-voiding lesions in the esophageal background mucosa. *J Gastroenterol Hepatol* 2019; **34:** 390–396.

SUPPLEMENTARY MATERIAL ONLINE

Supplementary materials and methods

Figure S1. Immunohistochemical staining in early oesophageal squamous cell carcinoma (ESCC) tissues using normal rabbit IgG, anti-integrin β4 (β4) antibody, and anti-β4 antibody with β4-blocking peptide

Figure S2. Characteristics of various polarised peripheral blood monocyte-derived macrophages

Figure S3. Phosphokinase expression profile of the protein from Het-1A monoculture and Het-1A co-cultured with M0 macrophages (co-M0), M1 macrophages (co-M1), and M2 macrophages (co-M2)

Figure S4. Cytokine expression profile of the condition medium from Het-1A and M2 macrophages (M2) monoculture and Het-1A co-cultured with M2

Figure S5. YKL-40/osteopontin (OPN) promoted the proliferation and migration of oesophageal epithelial cells via the mTOR–p70S6K signalling pathway

Figure S6. YKL-40 and osteopontin (OPN) promoted the proliferation and migration of Het-1A, TE-9, and TE-11 cells via the mTOR–p70S6K signalling pathway

Figure S7. The co-localization between YKL-40 or osteopontin (OPN) and integrin β4 (β4) and intensity of β4 on Het-1A cells co-cultured with M2 macrophages (M2) for 24 h were increased compared with monocultured Het-1A cells

Figure S8. YKL-40/osteopontin (OPN) promoted the proliferation and migration of oesophageal epithelial cells by activating the mTOR–p70S6K signalling pathway via integrin β4 (β4)

Figure S9. Immunohistochemical analysis of infiltrating immune cells and tumour cells in oesophagus tissues of the mouse oesophageal carcinogens model

Figure S10. Immunohistochemical analysis of infiltrating immune cells and tumour cells in early oesophageal squamous cell carcinoma (ESCC) tissues

Figure S11. Quantification of western blotting bands on the mTOR–p70S6K signalling pathway

Table S1. Correlation between the expression levels of integrin β4 (β4) and phosphorylated p70S6K (p-p70S6K) and infiltrating cells in oesophageal squamous cell carcinoma (ESCC) tissues

Table S2. Correlation between the numbers of infiltrating YKL-40- and osteopontin (OPN)-positive cells and clinicopathological parameters in early oesophageal squamous cell carcinoma (ESCC)

Table S3. Characteristics of patients and oesophageal squamous cell carcinoma (ESCC) tissues (referred to in Supplementary materials and methods)

Table S4. Experimental materials and the primer sets used for RT-qPCR (referred to in Supplementary materials and methods)